JOURNAL OF
MOLECULAR
CATALYSIS
A: CHEMICAL

Photoinduced hydrogen evolution with bisviologen-linked ruthenium(II) complexes and hydrogenase

Tomohiro Hiraishi, Toshiaki Kamachi, Ichiro Okura [*]

Department of Bioengineering, Tokyo Institute of Technology, Nagatsuta-cho 4259, Midori-ku, Yokohama 226-8501, Japan

Abstract

Bisviologen-linked ruthenium(II) complexes with different methylene chain length between ruthenium complex and viologen, $Ru(bpy)_2(dcbpy)C_mV_AC_nV_B$ ($m = 2$, $n = 3$; $m = 3$, $n = 4$), were synthesized and characterized. From luminescence spectra, the photoexcited state of $Ru(bpy)_2(dcbpy)$ moiety is oxidatively quenched by the bound viologen, and an intramolecular electron transfer occurs. Luminescence lifetime measurements show that the electron transfers from the photoexcited state of ruthenium(II) complex moiety to the bound bisviologen more rapidly than that of monoviologen-linked ruthenium(II) complexes. $Ru(bpy)_2(dcbpy)C_mV_AC_nV_B$ were applied to the photoinduced hydrogen evolution in the system containing nicotinamide-adenine dinucleotide phosphate (reduced form, NADPH), $Ru(bpy)_2(dcbpy)C_mV_AC_nV_B$ and hydrogenase under steady state irradiation. In the case of $Ru(bpy)_2(dcbpy)C_3V_AC_4V_B$, the efficient photoinduced hydrogen evolution was observed. © 2000 Elsevier Science B.V. All rights reserved.
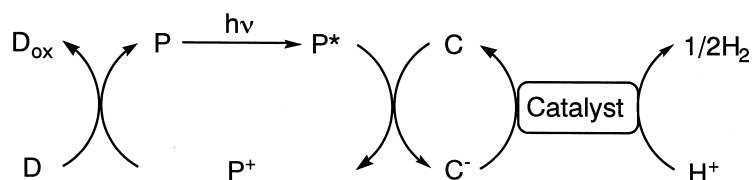
Keywords: Photoinduced hydrogen evolution; Bisviologen-linked ruthenium(II) complexes; Hydrogenase; Intramolecular electron transfer

1. Introduction

Photoinduced hydrogen evolution from water has been studied extensively using a system composed of four components: electron donor (D), photosensitizer (P), electron carrier (C) and catalyst as shown in Scheme 1 [1–4]. Among inorganic photosensitizers, ruthenium tris(2,2′-bipyridine) derivatives are the suitable compounds for photoinduced hydrogen evolution system, because ruthenium complexes possess properties such as photostability in water, high

extinction coefficients in the visible region, and relatively long-lived excited states. In this reaction, the reduction of electron carrier is one of the important steps. In the four-component system, however, the diffusional electron transfer step from photoexcited photosensitizer to electron carrier occurs leading to the low yield of charge separation state. To improve this system, the longer lifetimes of charge separated states between photosensitizer and electron carrier are desired. Charge separation processes have been extensively studied in acceptor-linked photosensitizer systems [5–15]. In these artificial systems, such as a viologen-linked ruthenium(II) complex, the intramolecular electron transfer

[*] Corresponding author. Tel.: +81-045-9245752; fax: +81-045-9245778; E-mail: iokura@bio.titech.ac.jp
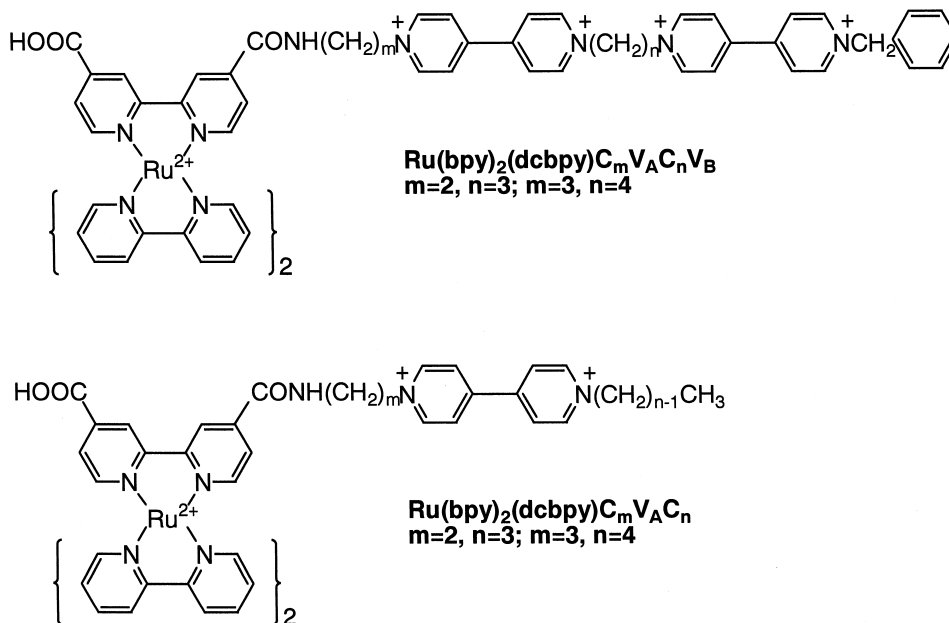
Scheme 1. Photoinduced hydrogen evolution system.

from ruthenium complex moiety to binding viologen competes with the rapid back electron transfer from acceptor to photosensitizer leading to the shortlived charge separated state [12–14]. To achieve the long-lived charge separated states in the model systems, the suppression of the back electron transfer is required. The charge separation is stabilized by a multistep electron transfer in a series of acceptors arranged in a fashion analogous to the electron transfer chain in photoreaction center. Among the viologen-linked ruthenium complexes, bisviologen-linked ruthenium complexes, in which two viologens with different redox potentials are connected covalently, are suitable compounds to establish

the effective photoinduced hydrogen evolution system, because photoinduced two-step electron transfer from photoexcited ruthenium complex moiety to acceptor may occur, and back electron transfer is suppressed.

In this paper, bisviologen-linked ruthenium (II) complexes, $Ru(bpy)_2(dcbpy)C_mV_AC_nV_B$ ($m = 2$, $n = 3$; $m = 3$, $n = 4$), (the structures are shown in Fig. 1), were synthesized and characterized by spectroscopic measurements. As the reduction of NADP to NADPH occurs with the concomitant oxygen evolution in photosynthesis, NADPH was used as an electron donor in the artificial photoinduced hydrogen evolution system. Bisviologen-linked ruthenium(II) com-

Fig. 1. Structures of $Ru(bpy)_2(dcbpy)C_mV_AC_nV_B$ and $Ru(bpy)_2(dcbpy)C_mV_AC_n$.

plexes were applied to photoinduced hydrogen evolution system containing NADPH, Ru (bpy)$_2$(dcbpy)C$_m$V$_A$C$_n$V$_B$ and hydrogenase.

2. Materials and methods

2.1. Materials

All reagents were of analytical or of the highest grade available. 4,4′-Dimethyl-2,2′-bipyridine (dmbpy), 4,4′-dicarboxy-2,2′-bipyridine (dcbpy), bisviologen-linked 4-carboxy-2,2′-bipyridine-4′-carbodiimide ((dcbpy)C$_m$V$_A$C$_n$V$_B$) and Ru(bpy)$_2$Cl$_2$ · nH$_2$O were prepared as described previously [16–19].

2.2. Preparation of bis- and monoviologen-linked ruthenium(II) complexes

The tris(bipyridyl)ruthenium(II) complexes were prepared by refluxing Ru(bpy)$_2$Cl$_2$ · nH$_2$O with either (dcbpy)C$_3$V$_A$C$_4$V$_B$ or (dcbpy)-C$_2$V$_A$C$_3$V$_B$ in 1:1 EtOH:H$_2$O under argon. The reaction was monitored by UV–vis spectroscopy. The Ru(II) complexes were applied to a neutral alumina column to remove the impurity and starting material (1:1 acetone:ethanol). The product was eluted as a orange band with methanol eluent. After removal of solvent under vacuum, the orange compound was dissolved in 25 mmol dm^{-3} Tris–HCl buffer (Tris, tris(hydroxymethyl)aminomethane) (pH 7.4) and applied to a SP Sepharose Fast Flow cation exchange column (Pharmacia). The desired product was eluted with a linear gradient from 0 to 1 mol dm^{-3} NaCl as a single peak. Monoviologen-linked ruthenium(II) complexes (Ru-(bpy)$_2$(dcbpy)C$_m$V$_A$C$_n$) were synthesized analogously to the preparation of bisviologen-linked ruthenium(II) complexes.

2.3. Purification of hydrogenase

Hydrogenase was purified from *Desulfovibrio vulgaris* (Miyazaki) according to the litera-

ture [20]. Protein concentration was determined using the following molar absorption coefficient: $\varepsilon = 155$ mmol^{-1} dm^3 cm^{-1} at 280 nm.

2.4. Spectroscopic measurements

UV–vis absorption spectra were measured in 25 mmol dm^{-3} Tris–HCl buffer (pH 7.4) using a Shimadzu MultiSpec-1500 spectrometer.

^{1}H-NMR spectra were recorded on a Varian GEMINI-200. The chemical shifts were referenced to the solvent peak calibrated against tetramethylsilane (TMS).

The luminescence spectra were measured in 25 mmol dm^{-3} Tris–HCl buffer (pH 7.4) at room temperature using a Hitachi F-4000 spectrometer. The absorbance at the excitation wavelength was kept constant at 0.3 for all the sample solutions in these experiments.

Luminescence lifetime measurements were carried out by using time-correlated single-photon-counting (Horiba NAES-500 spectrometer) under argon.

2.5. Photoinduced hydrogen evolution under steady state irradiation

For the steady-state irradiation, the sample solution in a Pyrex cell was irradiated using 200 W tungsten lamp (Philips KP-8) at 30°C. Light of wavelength less than at 390 nm was removed by Toshiba L-39 cut-off filter. The sample solution containing NADPH (2.0 mmol dm^{-3}), Ru(bpy)$_2$(dcbpy)C$_m$V$_A$C$_n$V$_B$ (10 μmol dm^{-3}) and hydrogenase (0.15 μmol dm^{-3}) in 3.0 ml of 25 mmol dm^{-3} Tris–HCl buffer (pH 7.4) was deaerated by repeated freeze-pump-thaw cycles and then incubated for 5 min under argon. Evolved hydrogen was detected by gas chromatography (Shimadzu GC-14B, detector: TCD, column: active carbon).

2.6. Determination of kinetic parameters

Hydrogen evolution was measured in the presence of dithionite-reduced Ru(bpy)$_2$-

$(dcbpy)C_mV_AC_nV_B$ in a 5-ml test tube sealed with Septa at 30°C under argon. The sample solutions contained $Ru(bpy)_2(dcbpy)C_mV_AC_nV_B$ and dithionite (20 mmol dm^{-3}) in 4 ml of 25 mmol dm^{-3} Tris–HCl buffer (pH 7.4). The reaction was started by injecting a small volume of hydrogenase solution (final conc.; 37 nmol dm^{-3}).

3. Results and discussion

3.1. Photophysical properties of $Ru(bpy)_2$-$(dcbpy)C_mV_AC_nV_B$ and $Ru(bpy)_2(dcbpy)C_mv_AC_n$

The absorption maxima of $Ru(bpy)_2$-$(dcbpy)C_mV_AC_nV_B$, $Ru(bpy)_2(dcbpy)C_mV_AC_n$ and $Ru(bpy)_2(dcbpy)$ are listed in Table 1. As an example, the absorption spectra of Ru$(bpy)_2(dcbpy)C_3V_AC_4V_B$, $Ru(bpy)_2(dcbpy)$ $C_3V_AC_4$ and $Ru(bpy)_2(dcbpy)$ are shown in Fig. 2. The absorption spectra of Ru$(bpy)_2(dcbpy)C_mV_AC_nV_B$ and $Ru(bpy)_2$ $(dcbpy)C_mV_AC_n$ are similar to that of $Ru(bpy)_2(dcbpy)$, with exception of the slightly broadening of MLCT band. Launikonis et al. [21] reported that the substitution of bpy to dcbpy leads to the broadening of MLCT band in ruthenium complexes. In the $Ru(bpy)_2$-$(dcbpy)C_mV_AC_nV_B$ and $Ru(bpy)_2(dcbpy)$-$C_mV_AC_n$, MLCT band may be broaden due to the substitution of dcbpy to $(dcbpy)C_mV_AC_nV_B$. From the absorption spectra, no electronic inter-
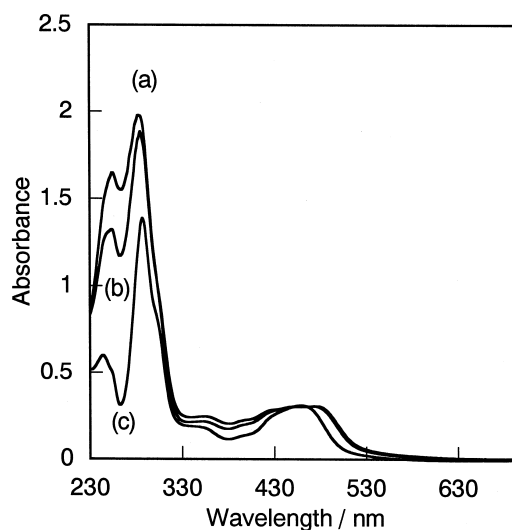

Fig. 2. Absorption spectra of $Ru(bpy)_2(dcbpy)C_3V_AC_4V_B$ (a), $Ru(bpy)_2(dcbpy)C_3V_AC_4$ (b) and $Ru(bpy)_2(dcbpy)$ (c) in 25 mmol dm^{-3} Tris–HCl buffer (pH 7.4).

action between the $Ru(bpy)_2(dcbpy)$ site and the bound bisviologen may occur in the ground state. The absorption maximum of the dithionite-reduced $Ru(bpy)_2(dcbpy)C_mV_AC_nV_B$ was at 540 nm (data not shown). In the case of the reduced $Ru(bpy)_2(dcbpy)C_mV_AC_n$, the absorption maximum was at 605 nm. These results suggest that the intramolecular interaction between V_A and V_B may occur. Similar observation was demonstrated by Atherton et al. [22]. It was examined that the intramolecular association of covalently linked viologen radical via methylene chain occurred.

The photoexcited states of $Ru(bpy)_2$-$(dcbpy)C_mV_AC_nV_B$ and $Ru(bpy)_2(dcbpy)C_m$-V_AC_n were studied using the luminescence emission spectra. As an example, the luminescence spectra of $Ru(bpy)_2(dcbpy)C_3V_AC_4V_B$, Ru$(bpy)_2(dcbpy)C_3V_AC_4$ and $Ru(bpy)_2(dcbpy)$ are shown in Fig. 3. For $Ru(bpy)_2(dcbpy)C_mV_A$-C_nV_B, the shapes of the luminescence spectra of $Ru(bpy)_2(dcbpy)C_mV_AC_nV_B$ were the same as that of $Ru(bpy)_2(dcbpy)$. However, the luminescence intensity of $Ru(bpy)_2(dcbpy)C_mV_AC_nV_B$ was lower than that of $Ru(bpy)_2(dcbpy)$. This result indicates that the photoexcited state of

Table 1
Wavelength of absorption maxima of $Ru(bpy)_2(dcbpy)$ $C_mV_AC_nV_B$, $Ru(bpy)_2(dcbpy)C_mV_AC_n$ and $Ru(bpy)_2(dcbpy)$

Compound	Wavelength of absorption maxima (nm)		
$Ru(bpy)_2(dcbpy)$	244	287	458
$Ru(bpy)_2(dcbpy)C_2V_AC_3$	249	285	452
$Ru(bpy)_2(dcbpy)C_3V_AC_4$	254	285	454
$Ru(bpy)_2(dcbpy)C_2V_AC_3V_B$	255	284	454
$Ru(bpy)_2(dcbpy)C_3V_AC_4V_B$	255	283	455
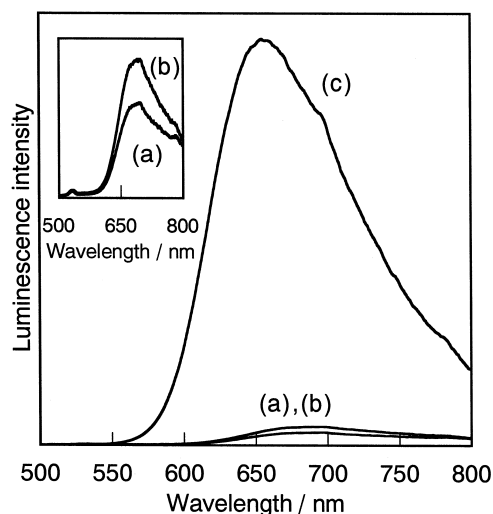
Fig. 3. Luminescence spectra of Ru(bpy)$_2$(dcbpy)C$_3$V$_A$C$_4$V$_B$ (a), Ru(bpy)$_2$(dcbpy)C$_3$V$_A$C$_4$ (b) and Ru(bpy)$_2$(dcbpy) (c) in 25 mmol dm^{-3} Tris–HCl buffer (pH 7.4). The excitation wavelength was 450 nm. Inset shows the magnified Y-axis of Fig. 3.

Ru(bpy)$_2$(dcbpy) site is oxidatively quenched by the bound bisviologen due to an intramolecular electron transfer and no electronic interaction occurs between the Ru(bpy)$_2$(dcbpy) moiety and the bound bisviologen in the photoexcited state. In addition, the intensity of Ru(bpy)$_2$(dcbpy)C$_m$V$_A$C$_n$V$_B$ was lower than that of Ru(bpy)$_2$-(dcbpy)C$_m$V$_A$C$_n$, indicating that the photoexcited ruthenium complex moiety in Ru(bpy)$_2$-(dcbpy)C$_m$V$_A$C$_n$V$_B$ is more efficiently quenched than that in Ru(bpy)$_2$(dcbpy)C$_m$V$_A$C$_n$.

3.2. Luminescence lifetimes of Ru(bpy)$_2$-(dcbpy)C$_m$V$_A$C$_n$V$_B$

The photoexcited state lifetime of Ru(bpy)$_2$-(dcbpy)C$_m$V$_A$C$_n$V$_B$ was measured by time-correlated single photon counting. The results are listed in Table 2. As an example, the luminescence decays of Ru(bpy)$_2$(dcbpy)C$_3$V$_A$C$_4$V$_B$ and Ru(bpy)$_2$(dcbpy)C$_3$V$_A$C$_4$ are shown in Fig. 4. For Ru(bpy)$_2$(dcbpy), the luminescence decay was first order kinetics and the excited lifetime was determined as 507 ns. For the mono- and bisviologen-linked ruthenium complexes, the luminescence decays of Ru(bpy)$_2$(dcbpy)C$_m$V$_A$C$_n$V$_B$ and Ru(bpy)$_2$(dcbpy) C$_m$V$_A$C$_n$ were much shorter than that of Ru(bpy)$_2$(dcbpy) due to the quenching of photoexcited Ru(bpy)$_2$(dcbpy) moiety by the bound viologen. This result also indicates that the oxidative quenching of photoexcited state of Ru (bpy)$_2$(dcbpy) site is the major deactivation pathway of the photoexcited state. In the case of mono- and bisviologen-linked ruthenium complexes, the decays obeyed double exponential kinetics. The reason of two components of lifetime is explained as follows. For the mono- and bisviologen-linked ruthenium complexes, there may be two conformers. In quinone-linked porphyrins and viologen-linked porphyrins, two conformers are proposed by Siemiarczuk et al. [23] and Batteas et al. [24]. The proposed conformation is as follows. The fast process may be attributed to electron transfer between proximal partners. In this conformation, the acceptor is held in close proximity to porphyrin, so that rapid process occurs. On the other hand, the slow process may be associated with conformation in which the bound acceptor is kept some distance away from the porphyrin.

The shorter component of photoexcited lifetimes (τ_s) of Ru(bpy)$_2$(dcbpy)C$_m$V$_A$C$_n$V$_B$ is shorter than that of Ru(bpy)$_2$(dcbpy)C$_m$V$_A$C$_n$, indicating that the photoexcited ruthenium complex moiety in Ru(bpy)$_2$(dcbpy)C$_m$V$_A$C$_n$V$_B$ is

Table 2

Luminescence lifetimes of Ru(bpy)$_2$(dcbpy)C$_m$V$_A$C$_n$V$_B$ and Ru(bpy)$_2$(dcbpy) C$_m$V$_A$C$_n$

Compound	τ_{mono} (10^{-9} s)	τ_{bis} (10^{-9} s)
Ru(bpy)$_2$(dcbpy)C$_2$V$_A$C$_3$	τ_s: 3.9 (86%), τ_1: 11.6 (14%)	
Ru(bpy)$_2$(dcbpy)C$_3$V$_A$C$_4$	τ_s: 3.7 (83%), τ_1: 18.6 (17%)	
Ru(bpy)$_2$(dcbpy)C$_2$V$_A$C$_3$V$_B$		τ_s: 1.5 (86%), τ_1: 6.9 (14%)
Ru(bpy)$_2$(dcbpy)C$_3$V$_A$C$_4$V$_B$		τ_s: 1.2 (76%), τ_1: 20.9 (24%)

Fig. 4. Luminescence decays of $Ru(bpy)_2(dcbpy)C_3V_AC_4V_B$ (a) and $Ru(bpy)_2(dcbpy)C_3V_AC_4$ (b) in 25 mmol dm^{-3} Tris–HCl buffer (pH 7.4). The excitation wavelength was 350 nm.

quenched by V_A and V_B as shown in Scheme 2, where Ru^{2+} represents $Ru(bpy)_2(dcbpy)$ moiety.

From Scheme 2, the intramolecular electron transfer rate constants (k_{oq1}, k_{oq2}) can be determined from the measured lifetime of photoexcited ruthenium complexes according to Eqs. (1) and (2).

$$k_{bis} = k_{oq1} + k_{oq2} = \frac{1}{\tau_{bis,s}} - \frac{1}{\tau_d} \qquad (1)$$

$$k_{oq1} = \frac{1}{\tau_{mono,s}} - \frac{1}{\tau_d} \qquad (2)$$

where τ_d is the excited state lifetime of the viologen free ruthenium(II) complex. $\tau_{mono,s}$ and $\tau_{bis,s}$ are the shorter components of excited state lifetimes of the mono- and bisviologen-linked

Scheme 2.

Table 3
Intramolecular electron transfer rates of $Ru(bpy)_2$ (dcbpy)-$C_mV_AC_nV_B$ and $Ru(bpy)_2(dcbpy)C_mV_AC_n$

Compound	k_{oq1} (10^8 s^{-1})	k_{oq2} (10^8 s^{-1})
$Ru(bpy)_2(dcbpy)C_2V_AC_3$	2.54	
$Ru(bpy)_2(dcbpy)C_3V_AC_4$	2.68	
$Ru(bpy)_2(dcbpy)C_2V_AC_3V_B$	2.54	4.10
$Ru(bpy)_2(dcbpy)C_3V_AC_4V_B$	2.68	5.63

ruthenium complexes, respectively. The apparent intramolecular electron transfer rate (k_{bis}) in $Ru(bpy)_2(dcbpy)C_mV_AC_nV_B$ represents as follows, $k_{bis} = k_{oq1} + k_{oq2}$. As the k_{oq1} value is the same as the intramolecular electron transfer rate in $Ru(bpy)_2(dcbpy)C_mV_AC_n$, k_{oq1} represents as shown in Eq. (2). The intramolecular electron transfer rate constants are given in Table 3.

The electrochemical measurements showed that the two step electron transfer from the photoexcited state of ruthenium complex to bisviologen may occur [18]. On the other hand, the luminescence lifetime measurements suggest that the electron transfers from the photoexcited ruthenium complex moiety to V_A and V_B. These results indicate that the two step electron transfer may occur with the concomitant electron transfer from the photoexcited state of ruthenium complex moiety to V_A and V_B.

3.3. Photoreduction of bound viologen in $Ru(bpy)_2(dcbpy)C_mV_AC_nV_B$

When the solution containing NADPH and $Ru(bpy)_2(dcbpy)C_mV_AC_nV_B$ was irradiated, the absorbance due to reduced bisviologen increased. As an example, the absorption spectrum change of $Ru(bpy)_2(dcbpy)C_3V_AC_4V_B$ at 540 nm is shown in Fig. 5. The reaction was completed within 6 min. On the other hand, when $Ru(bpy)_2(dcbpy)C_mV_AC_n$ was used, no reduction of the bound viologen was observed. These results suggest that the bound bisviologen in $Ru(bpy)_2(dcbpy)C_mV_AC_nV_B$ molecule is more easily reduced than that in $Ru(bpy)_2$-$(dcbpy)C_mV_AC_n$ due to the suppression of the

Fig. 5. Time dependence of the absorption change of $Ru(bpy)_2(dcbpy)C_3V_AC_4V_B$ under steady-state irradiation monitored at 540 nm. The solution contains 2.0 mmol dm^{-3} of NADPH and 10 μmol dm^{-3} of $Ru(bpy)_2(dcbpy)C_3V_AC_4V_B$ in 25 mmol dm^{-3} Tris–HCl buffer (pH 7.4).
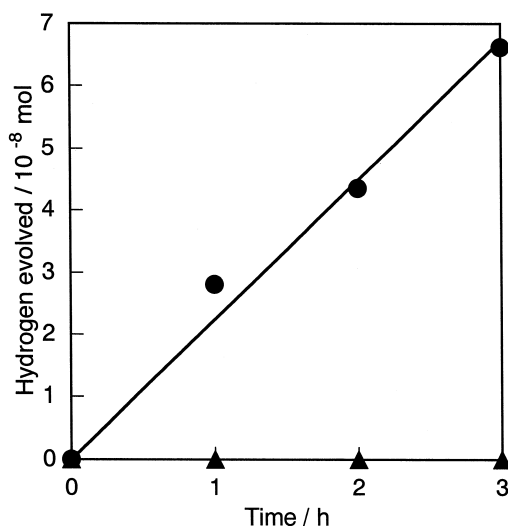

Fig. 6. Time dependence of photoinduced hydrogen evolution under steady state irradiation. The solution contains 2.0 mmol dm^{-3} of NADPH, 10 μmol dm^{-3} of $Ru(bpy)_2(dcbpy)C_3V_AC_4V_B$ and 0.15 μmol dm^{-3} of hydrogenase in 25 mmol dm^{-3} Tris–HCl buffer (pH7.4) (●). For the monoviologen linked ruthenium complex system, the solution contains 2.0 mmol dm^{-3} of NADPH, 10 μmol dm^{-3} of $Ru(bpy)_2(dcbpy)C_3V_AC_4$ and 0.15 μmol dm^{-3} of hydrogenase (▲).

back electron transfer from reduced viologen to the ruthenium complex moiety.

3.4. Photoinduced hydrogen evolution with hydrogenase

When the solution containing NADPH, $Ru(bpy)_2(dcbpy)C_3V_AC_4V_B$ and hydrogenase was irradiated, the photoinduced hydrogen evolution was observed. Fig. 6 shows the time dependence of the photoinduced hydrogen evolution. In the case of $Ru(bpy)_2(dcbpy)$-$C_2V_AC_3V_B$, however, no photoinduced hydrogen evolution was observed. For Ru$(bpy)_2(dcbpy)C_2V_AC_3V_B$, as the distance between $Ru(bpy)_2(dcbpy)$ moiety and the bound viologen is shorter than that of $Ru(bpy)_2$-$(dcbpy)C_3V_AC_4V_B$, the steric hindrance of Ru$(bpy)_2(dcbpy)C_2V_AC_3V_B$ may be larger than that of $Ru(bpy)_2(dcbpy)C_3V_AC_4V_B$. This result indicates that $Ru(bpy)_2(dcbpy)C_3V_AC_4V_B$ may be the more suitable substrate for hydrogenase than $Ru(bpy)_2(dcbpy)C_2V_AC_3V_B$. By using the system containing NADPH, $Ru(bpy)_2(dcbpy)$-$C_3V_AC_4V_B$ and hydrogenase, the effective pho-

toinduced hydrogen evolution was accomplished compared with the $Ru(bpy)_2(dcbpy)C_m$-V_AC_n system.
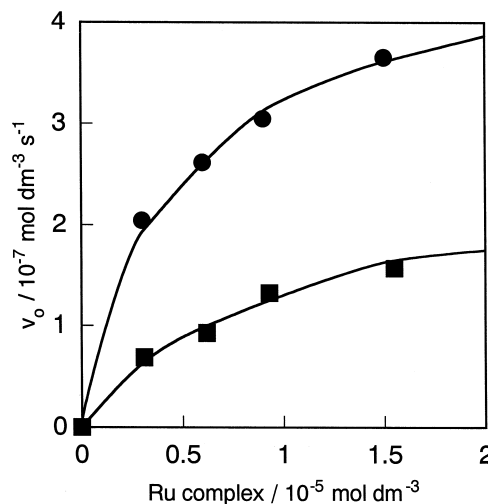

Fig. 7. Dependence of hydrogen evolution rate on the concentration of dithionite-reduced $Ru(bpy)_2(dcbpy)C_mV_AC_nV_B$ (■: $m = 2$, $n = 3$; ●: $m = 3$, $n = 4$). The sample solutions contains $Ru(bpy)_2(dcbpy)C_mV_AC_nV_B$, dithionite (20 mmol dm^{-3}) and hydrogenase (37 nmol dm^{-3}) in 4.0 ml of 25 mmol dm^{-3} Tris–HCl (pH 7.4).
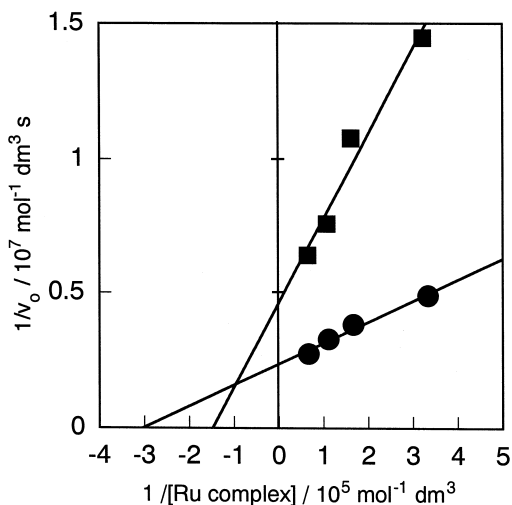
Fig. 8. Lineweaver–Burk plot for hydrogen evolution rate of hydrogenase with dithionite-reduced $Ru(bpy)_2(dcbpy)C_mV_AC_nV_B$ (■: $m = 2$, $n = 3$; ●: $m = 3$, $n = 4$).

3.5. Substrate affinity of $Ru(bpy)_2$-$(dcbpy)C_mV_aC_nV_B$ for hydrogenase

For the more detailed information on photoinduced hydrogen evolution using $Ru(bpy)_2(dcbpy)C_mV_AC_nV_B$ and hydrogenase, kinetic studies were carried out. In the presence of dithionite-reduced $Ru(bpy)_2(dcbpy)C_mV_A$-C_nV_B, hydrogen evolution with hydrogenase was observed. Hydrogen evolved linearly with reaction time. Fig. 7 shows the dependence of the initial rate of hydrogen evolution on the concentration of dithionite-reduced $Ru(bpy)_2$-$(dcbpy)C_mV_AC_nV_B$. The initial rate of hydrogen evolution increased with increasing the concentration of $Ru(bpy)_2(dcbpy)C_mV_AC_nV_B$ and reached constant values. In the system containing dithionite-reduced $Ru(bpy)_2(dcbpy)$-$C_mV_AC_nV_B$ and hydrogenase, the substrate affinity constants (K_m), maximum velocity (V_{max}), catalytic constants (k_{cat}) and catalytic efficiency (k_{cat}/K_m) were determined from the double reciprocal plots as shown in Fig. 8. The results are listed in Table 4. The k_{cat}/K_m value of $Ru(bpy)_2(dcbpy)C_3V_AC_4V_B$ is higher than that of $Ru(bpy)_2(dcbpy)C_2V_AC_3V_B$, indicating that $Ru(bpy)_2(dcbpy)C_3V_AC_4V_B$ is more suitable compound for hydrogen evolution than $Ru(bpy)_2(dcbpy)C_2V_AC_3V_B$. From these results, as $Ru(bpy)_2(dcbpy)C_3V_AC_4V_B$ has high affinity for hydrogenase compared with $Ru(bpy)_2(dcbpy)C_2V_AC_3V_B$, the efficient hydrogen evolution proceeded by using $Ru(bpy)_2(dcbpy)C_3V_AC_4V_B$. This result coincides with that of photoinduced hydrogen evolution in the system containing $Ru(bpy)_2(dcbpy)C_mV_AC_nV_B$ and hydrogenase. In the case of $Ru(bpy)_2(dcbpy)C_3V_AC_4V_B$, as the distance between the ruthenium complex moiety and the bound viologen is long enough, the bound viologen can be easily away from the ruthenium complex moiety leading to the higher affinity for hydrogenase by little steric hindrance among the ruthenium complex moiety, the bound viologen and hydrogenase. In the case of $Ru(bpy)_2(dcbpy)C_2V_AC_3V_B$, on the other hand, as the distance between ruthenium complex moiety and the bound viologen is short, the approach of bound viologen to ruthenium complex moiety may be more easily than that of $Ru(bpy)_2(dcbpy)C_3V_AC_4V_B$, so that steric hindrance is large.

Table 4
Kinetic parameters for hydrogen evolution with dithionite-reduced bisviologen linked ruthenium complexes and hydrogenase

Substrate	K_m (10^{-6} mol dm^{-3})	V_{max} (10^{-7} mol dm^{-3} s^{-1})	k_{cat} (s^{-1})	k_{cat}/K_m (10^5 mol^{-1} dm^3 s^{-1})
$Ru(bpy)_2(dcbpy)C_2V_AC_3V_B$	6.77	2.16	5.87	8.67
$Ru(bpy)_2(dcbpy)C_3V_AC_4V_B$	3.30	4.24	11.5	34.8

The kinetic parameters were determined by fitting to the Michaelis–Menten equation.

Acknowledgements

References

[1] J.R. Darwent, P. Douglas, A. Harriman, G. Porter, M.C. Richoux, Coord. Chem. Rev. 44 (1982) 93.

[2] J. Kiwi, K. Kalyanasundaram, M. Graetzel, Struct. Bonding 49 (1981) 37.

[3] I. Okura, Coord. Chem. Rev. 68 (1985) 53.

[4] I. Okura, S. Aono, A. Yamada, J. Phys. Chem. 89 (1985) 1593.

[5] M.R. Wasielewski, Chem. Rev. 92 (1992) 435.

[6] A. Osuka, S. Nakajima, K. Maruyama, N. Mataga, T. Asahi, I. Yamazaki, Y. Nishimura, T. Ohno, K. Nozaki, J. Am. Chem. Soc. 115 (1993) 4577.

[7] M. Ohkohchi, A. Takahashi, N. Mataga, T. Okada, A. Osuka, H. Yamada, K. Maruyama, J. Am. Chem. Soc. 115 (1993) 12137.

[8] D. Gust, T.A. Moore, A.L. Moore, S.-J. Lee, E. Bittersmann, D.K. Luttrull, A.A. Rehms, J.M. DeGraziano, X.C. Ma, F. Gao, R.E. Belford, T.T. Trier, Science 248 (1990) 199.

[9] A. Osuka, S. Marumo, K. Maruyama, N. Mataga, Y. Tanaka, S. Taniguchi, T. Okada, I. Yamazaki, Y. Nishimura, Bull. Chem. Soc. Jpn. 68 (1995) 262.

[10] D. Kuciauskas, P.A. Liddell, S.-C. Hung, S. Lin, S. Stone, G.R. Seely, A.L. Moore, T.A. Moore, D. Gust, J. Phys. Chem. B 101 (1997) 429.

[11] Y. Amao, T. Hiraishi, I. Okura, J. Mol. Catal. A Chem. 126 (1997) 13.

[12] E.H. Yonemoto, R.L. Riley, Y.H. Kim, S.J. Atherton, R.H. Schmehl, T.E. Mallouk, J. Am. Chem. Soc. 114 (1992) 8081.

[13] L.A. Kelly, M.A.J. Rodgers, J. Phys. Chem. 98 (1994) 6386.

[14] T. Hiraishi, T. Kamachi, I. Okura, J. Mol. Catal. A Chem. 138 (1999) 107.

[15] T.J. Rutherford, F.R. Keene, Inorg. Chem. 36 (1997) 2872.

[16] G. Sprintschnik, H.W. Sprintschnik, P.P. Kirsch, D.G. Whitten, J. Am. Chem. Soc. 99 (1977) 4947.

[17] L.A. Kelly, M.A.J. Rodgers, J. Phys. Chem. 98 (1994) 6377.

[18] T. Hiraishi, T. Kamachi, I. Okura, J. Photochem. Photobiol. A Chem. 116 (1998) 119.

[19] D.P. Rillema, D.G. Taghdiri, D.S. Jones, C.D. Keller, L.A. Worl, T.J. Meyer, H.A. Levy, Inorg. Chem. 26 (1987) 578.

[20] T. Yagi, J. Biochem. 68 (1970) 649.

[21] A. Launikonis, P.A. Lay, A.W.-H. Mau, A.M. Sargeson, W.H.F. Sasse, Aust. J. Chem. 39 (1986) 1053.

[22] S.J. Atherton, K. Tsukahara, R.G. Wilkins, J. Am. Chem. Soc. 108 (1986) 3380.

[23] A. Siemiarczuk, A.R. McIntosh, T.-H. Ho, M.J. Stillman, K.L. Roach, A.C. Weedon, J.R. Bolton, J.S. Connolly, J. Am. Chem. Soc. 105 (1983) 7224.

[24] J.D. Batteas, A. Harriman, Y. Kanda, N. Mataga, A.K. Nowark, J. Am. Chem. Soc. 112 (1990) 126.